High Energy Physics and Nuclear Physics

Volume 16, Number 2

Two-Particle Pseudorapidity Correlations in pp Collisions at 400 GeV/c

Wang Shaoshun, Zhang Jie, Xiao Chenguo, Ye Yunxiu, Cheng Zhengdong, Zhang Xueqian, Luo Qi, Xu Wanli and Xiong Weijun

Department of Modern Physics, University of Science and Technology of China, Hefei, Anhui, China

The pseudorapidity distribution of charged particles produced in pp collisions at 400 GeV/c was measured by using LEBC films. The two-particle pseudorapidity correlations at fixed multiplicity were studied. The experimental data were fitted with cluster model. It was found that the average cluster multiplicities as well as the cluster decay widths vary slightly with charged multiplicity.

1. INTRODUCTION

In order to better understand the dynamic mechanism of multi-particle production in high energy collisions, besides the study of the charged particle multiplicity distribution at different rapidity region, measurement also has been made widely of various correlations among final state particles.

A great deal of hadron collision experimental results show short-range and long-range correlations among the final state particles. The short-range correlations revealed that the final state particles are produced grouping into clusters [1-9]. Namely, the multiple production process can be regarded as such that several clusters are formed first and then these clusters decay into final state particles. However, because two particle rapidity (pseudorapidity) correlation functions in inclusive experiments show long-range correlation, it is difficult to explain the experimental results. Analyses show that the two particle rapidity (pseudorapidity) correlations at fixed multiplicity depend only on short-range correlation and that trivial correlations can be eliminated [9,10].

Therefore, on the basis of the experimental work of the multiplicity distribution of charged particles produced in pp collisions at 400 GeV/c, we measured the pseudorapidity distribution for 1501 events of multiplicities 8-24 by using the LEBC films offered by CERN NA27 collaboration

Supported by the National Natural Science Foundation of China.
Received on July 29, 1991.

(detailed description of the measuring method can be found in Ref. [11]). The experimental data for the semi-inclusive pseudorapidity distribution in C.M.S. were obtained (see Fig. 1). The two particle correlation functions were calculated and the experimental results were fitted with the cluster model. Finally, a comparison between the experimental results and those of other energies was made.

2. TWO-PARTICLE PSEUDORAPIDITY CORRELATION FUNCTIONS

In high-energy interactions, most of the final state particles have low transverse momenta. It is expected that the final state particles have dynamical correlations primarily in the longitudinal phase space. It is thus common to study two-particle rapidity (pseudorapidity) correlations. In order to study these correlations at fixed multiplicity, we introduce two quantities, one is single particle density

$$\rho_n^1(\eta) = \frac{1}{\sigma_n}\frac{\mathrm{d}\sigma_n}{\mathrm{d}\eta}, \tag{1}$$

the other is two-particle density

$$\rho_n^2(\eta_1, \eta_2) = \frac{1}{\sigma_n}\frac{\mathrm{d}^2\sigma_n}{\mathrm{d}\eta_1 \mathrm{d}\eta_2}. \tag{2}$$

Here σ_n is the topological cross section of multiplicity n for non-single-diffractive processes. The pseudorapidity

$$\eta = -\ln \operatorname{tg}\frac{\theta_c}{2},$$

depends only on the C.M.S. production angle θ_c. At fixed multiplicity n, the single particle density $\rho_n^1(\eta)$ is proportional to the probability of finding a charged particle at pseudorapidity η region. The two particle pseudorapidity density $\rho_n^2(\eta_1, \eta_2)$ is proportional to the probability of finding a charged particle at η_1 region while finding another charged particle at η_2 region. In order to investigate the difference between the joint production and independent production for two particles, two-particle pseudorapidity correlation function

$$C_n(\eta_1, \eta_2) = \rho_n^2(\eta_1, \eta_2) - \rho_n^1(\eta_1)\rho_n^1(\eta_2) \tag{3}$$

is introduced. Usually, the normalized two-particle correlation function

$$R_n(\eta_1, \eta_2) = \frac{C_n(\eta_1, \eta_2)}{\rho_n^1(\eta_1)\rho_n^1(\eta_2)} = \frac{\rho_n^2(\eta_1, \eta_2)}{\rho_n^1(\eta_1)\rho_n^1(\eta_2)} - 1 \tag{4}$$

is also used. The advantage for using $R_n(\eta_1, \eta_2)$ is that most of experimental efficiencies can be set off. If there is no correlation between two particles, then

$$\rho_n^2(\eta_1, \eta_2) = \frac{n-1}{n}\rho_n^1(\eta_1)\rho_n^1(\eta_2), \tag{5}$$

namely

$$R_n(\eta_1, \eta_2) = -\frac{1}{n}.$$

The experimental results indicated that the correlation functions C_n or R_n are large for $\eta_1 = \eta_2$, and vary with $\Delta\eta = \eta_1 - \eta_2$. The correlation functions C_n or R_n for the pseudorapidity plateau

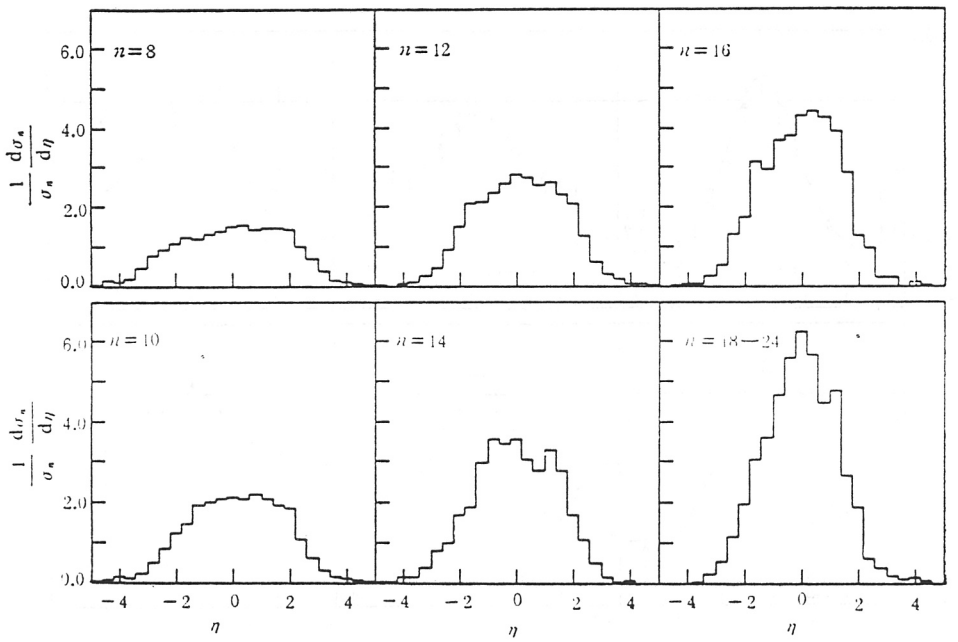

Fig. 1
The pseudorapidity distributions at fixed multiplicities in C.M.S..

region only depend on $|\eta_1 - \eta_2|$ and have no relation to the values of η_1 and η_2. For this reason the correlation functions can be expressed in the function of the pseudorapidity difference $\Delta\eta$. The correlation function $C_n(\eta, \eta + \Delta\eta)$ is integrated over the pseudorapidity plateau region and normalized. Then we obtain the new correlation function $R_n(\Delta\eta)$, namely

$$R_n(\Delta\eta) = \frac{\int_\eta \rho_n^2(\eta, \eta + \Delta\eta)\mathrm{d}\eta}{\int_\eta \rho_n^1(\eta) \cdot \rho_n^1(\eta + \Delta\eta)\mathrm{d}\eta} - 1, \tag{6}$$

which can use more information of the events, and can give most of information about $R_n(\eta_1, \eta_2)$. It can be seen from Fig. 1 that the widths of the pseudorapidity plateau regions are different for different multiplicities. Therefore, the integral regions should take different values, namely

$$\begin{aligned} &n = 8, 10, \quad |\eta| \leqslant 1.6, \quad |\eta + \Delta\eta| \leqslant 1.6; \\ &n = 12, 14, \quad |\eta| \leqslant 1.2, \quad |\eta + \Delta\eta| \leqslant 1.2; \\ &n \geqslant 16, \quad |\eta| \leqslant 1.05, \quad |\eta + \Delta\eta| \leqslant 1.05. \end{aligned} \tag{7}$$

Because the number of events for multiplicities 18-24 is small, they are added together in the analysis. At this time the two-particle correlation function is

$$R_r(\Delta\eta) = \frac{\int_\eta \rho_r^2(\eta, \eta + \Delta\eta)\mathrm{d}\eta}{\int_\eta \rho_r^1(\eta) \cdot \rho_r^1(\eta + \Delta\eta)\mathrm{d}\eta} - 1, \tag{8}$$

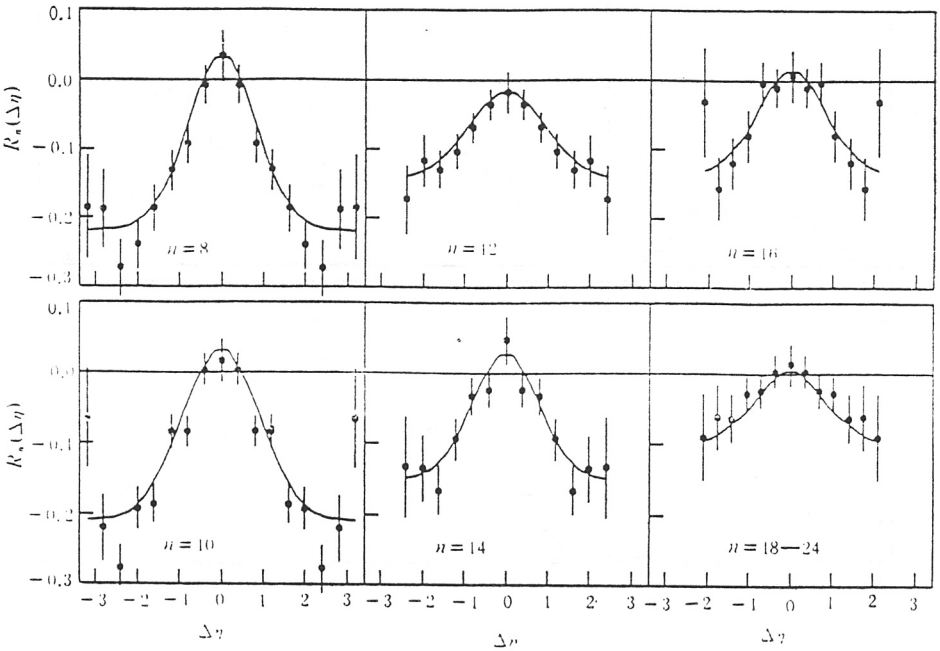

Fig. 2
The two-particle correlation functions at fixed multiplicity.

where

$$\rho_r^1(\eta) = \sum_n \pi(n)\rho_n^1(\eta), \tag{9}$$

$$\rho_r^2(\eta, \eta + \Delta\eta) = \sum_n \pi(n)\rho_n^2(\eta, \eta + \Delta\eta), \tag{10}$$

where r is the average multiplicity for this range of multiplicities, and $\pi(n)$ is the probability of multiplicity n. The experimental results are shown in Fig. 2, which clearly indicates the existence of short-range correlation.

3. EXPERIMENTAL RESULTS FITTED WITH CLUSTER MODEL

It is very successful to use cluster model to interpret the behavior of two-particle short-range correlations. In a simple cluster model, the final state particles are regarded as the product of cluster decay. A cluster at pseudorapidity η decays into K charged particles independently, their pseudorapidities being $\eta_i (i = 1, 2, \ldots, K)$ respectively. η_i follows the Gaussion distribution with mean value η and width δ. The selected events have fixed multiplicity n, and these n particles come from m clusters. The pseudorapidity of the cluster and cluster decay charged multiplicities are η_j and K_j $(j = 1, 2, \ldots, m)$, respectively. It is assumed that the decay width of the cluster δ_n is much smaller than the width of the pseudorapidity distribution of clusters. Then the two-particle correlation functions $R_n(\eta_1, \eta_2)$ can be fitted with function [9]

Table 1
The two cluster model parameters and mean cluster size obtained by fitting the experimental results with cluster model.

Multiplicity	8	10	12	14	16	18—24
$\left.\frac{\langle K(K-1)\rangle}{\langle K\rangle}\right\|_n$	0.76±0.10	1.11±0.13	0.76±0.19	1.14±0.23	1.24±0.33	1.12±0.40
δ_n	0.58	0.65	0.65	0.56	0.58	0.57
χ^2/NDF	0.58	1.85	0.24	0.53	0.58	0.27
K_c	1.76±0.10	2.11±0.13	1.76±0.19	2.14±0.23	2.24±0.33	2.12±0.40
$\langle K\rangle_{0n}$	0.93	1.17	0.71	0.98	1.00	0.83

$$R_n(\eta_1,\eta_2) = \frac{F_n \cdot \rho_n^1\left(\frac{\eta_1+\eta_2}{2}\right)}{\rho_n^1(\eta_1)\cdot\rho_n^1(\eta_2)} \frac{1}{2\sqrt{\pi}\,\delta_n} \cdot \exp\left[-\frac{(\eta_1-\eta_2)^2}{4\delta_n^2}\right] - \frac{1+F_n}{n} \tag{11}$$

where $F_n = \langle K(K-1)\rangle/\langle K\rangle|_n$. In our situation, the above formula should be changed into

$$R_n(\Delta\eta) = \frac{F_n \cdot \int_\eta \rho_n^1\left(\eta+\frac{\Delta\eta}{2}\right)d\eta}{\int_\eta \rho_n^1(\eta)\cdot\rho_n^1(\eta+\Delta\eta)d\eta} \frac{1}{2\sqrt{\pi}\,\delta_n} \cdot \exp\left[-\frac{(\Delta\eta)^2}{4\delta_n^2}\right] - \frac{1+F_n}{n}. \tag{12}$$

For the events of multiplicities 18-24, the following fitted formula should be used

$$R_r(\Delta\eta) = \frac{F_r \int_\eta \rho_r^1\left(\eta+\frac{\Delta\eta}{2}\right)d\eta}{\int_\eta \rho_r^1(\eta)\cdot\rho_r^1(\eta+\Delta\eta)d\eta} \frac{1}{2\sqrt{\pi}\,\delta_r} \cdot \exp\left[-\frac{(\Delta\eta)^2}{4\delta_r^2}\right] - \frac{1+F_r}{r} + \frac{\langle n^2\rangle - r^2}{r^2}, \tag{13}$$

the integral interval for η is the same as in Eq. (7). Here there are two adjustable parameters $\delta_n(\delta_r)$ and $F_n(F_r)$. The best values of the two parameters can be determined by the method of least squares.

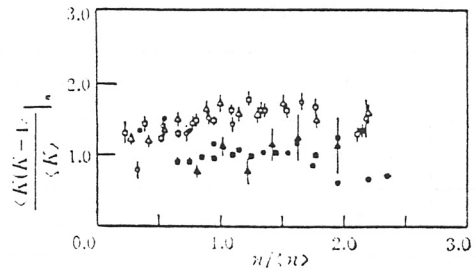

Fig. 3
The dependance of moment $<K(K-1)>/<K>|_n$ on multiplicities. △ UA5 900 GeV; □ UA5 546 GeV; ○ UA5 200 GeV; ■ PSB 63 GeV; ● SFM 44 GeV; ▲ This experiment 27.4 GeV.

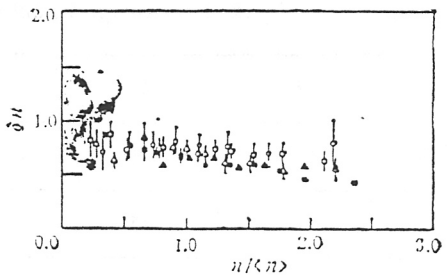

Fig. 4
The dependance of cluster decay width δ_n on multiplicities. △ UA5 900 GeV; □ UA5 546 GeV; ○ UA5 200 GeV; ● SFM 44 GeV; ▲ This experiment 27.4 GeV.

The fitted results are presented in Fig. 2 with curves. It can be seen from Fig. 2 that the simple cluster model can interpret the short-range correlation experimental results very well.

The values of δ_n and $<K(K-1)>/<K>|_n$ obtained by fitting experimental data are listed in Table 1. In Figs. 3 and 4, $<K(K-1)>/<K>|_n$ and δ_n for different energies are plotted versus $n/<n>$, respectively. The data for other energies are taken from Ref. [13]. It can be seen from Figs. 3 and 4 that the moments $<K(K-1)>/<K>|_n$ as well as δ_n have no significant charged multiplicity dependence.

The relation between the moment $<K(K-1)>/<K>|_n$ and average cluster size $<K>$ depends on the multiplicity distribution of the cluster decay. If this distribution is a δ-function, namely every cluster decays into a constant number of charged particles K_c, the mean value $<K>$ is

$$\langle K\rangle = K_c = \left.\frac{\langle K(K-1)\rangle}{\langle K\rangle}\right|_n + 1. \tag{14}$$

The calculated mean size of cluster from this equation is listed in Table 1. Averaged for different multiplicities, the mean cluster size is

$$<K> = 2.00 \pm 0.19.$$

If the cluster decay multiplicity distribution is a Poisson distribution with an average $<K>_0$, then we have [13]

$$\left.\frac{\langle K(K-1)\rangle}{\langle K\rangle}\right|_n = \frac{n-1}{n}\frac{\sigma_{n-1}}{\sigma_n}\langle K\rangle_0 = \frac{n-1}{n+k-1}\frac{\bar{n}+k}{\bar{n}}\langle K\rangle_0, \tag{15}$$

The right hand side of the relation is the result of the assumption that the charged particle multiplicity distribution for non-single-diffractive process is a negative binomial distribution. Based on the experimental result of multiplicity distribution [14],

$$k = 12.8, \bar{n} = 9.84$$

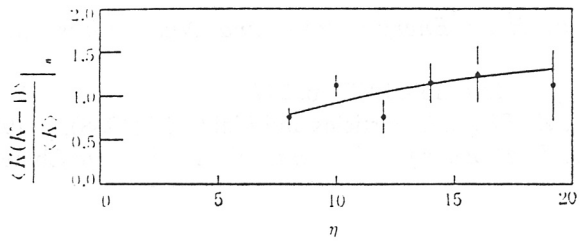

Fig. 5
The dependance of moment $<K(K-1)>/<K>|_n$ on n.

We therefore obtain $<K>_{0n}$ at fixed multiplicity. It is also listed in Table 1.

The relation (15) has been fitted to the experimental results with a free parameter $<K>_0$ as shown in Fig. 5. This yields $<K>_0 = 0.97 \pm 0.15$. Because $<K>_0$ includes the cluster which decays into exclusively neutral particles, namely $K = 0$, after excluding these clusters, we obtain the mean cluster size

$$<K> = 1.56 \pm 0.10.$$

To sum up, the average cluster size is $2.00 \geq <K> \geq 1.56$. A comparison of this result with the experimental result of the forward hemisphere multiplicity distribution [11] shows that the cluster decay multiplicity distribution is compatible with Poisson distribution.

4. CONCLUSIONS

The above results show two-particle pseudorapidity short-range correlations at fixed multiplicities. The cluster model can explain the experimental results of the short-range correlations very well. The two cluster model parameters $<K(K-1)>/<K>|_n$ and δ_n both vary slightly with n. A comparison of this result with the experimental result of forward hemisphere multiplicity distributions shows that the cluster decay multiplicity distribution is compatible with a Poisson distribution.

ACKNOWLEDGMENTS

The authors are grateful to CERN NA 27 collaboration for offering the LEBC films.

REFERENCES

[1] Berger, E. L., *Phys. Lett.*, **49B** (1974), p. 569.
[2] Foa, L., *Phys. Rep.*, **22** (1975), p. 1.
[3] Berger, E. L., *Nucl. Phys.*, **B85** (1975), p. 61.
[4] Eggert, K. *et al.*, *Nucl. Phys.*, **B86** (1975), p. 201.
[5] Whitemore, J., *Phys. Rep.*, **27** (1976), p. 187.
[6] Kafka, T. *et al.*, *Phys. Rev.*, **D16** (1977), p. 126.
[7] Drijard, D. *et al.*, *Nucl. Phys.*, **B155** (1979), p. 269.
[8] Giacomelli, G., and Jacob, M., *Phys. Rep.*, **55** (1979), p. 1.
[9] Bell, W. *et al.*, *Z. Phys.*, C-Particles and Fields, **22** (1984), p. 109.
[10] Mangotra, L. K. *et al.*, *Z. Phys.*, C-Particles and Fields, **31** (1986), p. 199.

[11] Wang Shaoshun *et al.*, *High Energy Phys. and Nucl. Phys.* (in Chinese), **15** (1991), p. 1057.
[12] Alner, G. J. *et al.*, *Phys. Rep.*, **154**(1987), p. 247.
[13] Ansorge, R. E. *et al.*, *Z. Phys.*, C-Particles and Fields, **37** (1988), p. 191.
[14] Wang Shaoshun *et al.*, *High Energy Phys. and Nucl. Phys.* (in Chinese), **13** (1989), p. 673.